Earth, Moon and Planets (2005) 97: 127–145
DOI 10.1007/s11038-006-9065-y

THE HILL PROBLEM WITH OBLATE SECONDARY: NUMERICAL EXPLORATION

A.E. PERDIOU, V.V. MARKELLOS and C.N. DOUSKOS
Department of Engineering Sciences, University of Patras, GR-26500 Patras, Greece
(E-mails: a.perdiou@des.upatras.gr; markellos@des.upatras.gr; c.douskos@des.upatras.gr)

(Received 31 July 2005; Accepted 9 January 2006)

Abstract. We introduce a three-dimensional version of Hill's problem with oblate secondary, determine its equilibrium points and their stability and explore numerically its network of families of simple periodic orbits in the plane, paying special attention to the evolution of this network for increasing oblateness of the secondary. We obtain some interesting results that differentiate this from the classical problem. Among these is the eventual disappearance of the basic family g' of the classical Hill problem and the existence of out-of-plane equilibrium points and a family of simple-periodic plane orbits non-symmetric with respect to the x-axis.

Keywords: equilibrium points, Hill problem, oblate secondary, periodic orbits, stability

1. Introduction

In several papers of recent years modifications of the classical restricted three-body problem have been employed to capture the effects of radiation and/or oblateness of the two massive bodies (e.g. Hamilton and Krivov, 1996; Oberti and Vienne, 2003; Gurfil and Meltzer, 2005, among others). As argued in Sharma (1987), perhaps the most relevant for Solar System applications is the case of a radiating spherical primary (the Sun) and/or an oblate non-radiating secondary (a major planet). With this consideration, in a previous paper in this journal (Kanavos et al., 2002) the photogravitational version of Hill's problem introduced in Markellos et al. (2000) was explored numerically in the case of radiating primary, with respect to its equilibrium points and its network of families of periodic orbits and their stability, among other features. The motivation for employing the Hill problem formulation, instead of the corresponding version of the restricted three-body problem, is to take advantage of the ensuing simplification in order to gain insight on the orbital behaviour of the massless particle moving in the vicinity of the secondary.

In the present paper we carry out a similar numerical exploration of the Hill problem with oblate secondary, introduced in its coplanar form in Markellos et al. (2001). Our aim is to consider the basic dynamical features

of this new model, rather than to pursue some particular astronomical application. In section 2 we present the equations of motion of the three dimensional case and in section 3 we determine its equilibrium points and their stability, while in section 4 we obtain analytical approximations of the coplanar Lyapunov orbits. In section 5 we explore numerically the network of families of simple periodic orbits in the plane and in particular the evolution of this network away from the classical Hill problem. We conclude by summarizing our results that characterize this model-problem and differentiate it from the classical Hill.

2. Equations of Motion

The Hill problem with oblate secondary, introduced here in its three-dimensional form, is derived from the restricted three-body problem with oblate secondary, in a similar way as the classical Hill problem is derived from the classical restricted problem, after some scale changes and a limiting process on the mass parameter $\mu = m_2/(m_1 + m_2) \to 0$. The restricted problem with oblate secondary is described by the following equations of motion, in rotating coordinates:

$$\ddot{X} - 2n\dot{Y} = \Omega_X, \qquad \ddot{Y} + 2n\dot{X} = \Omega_Y, \quad \ddot{Z} = \Omega_Z, \tag{1}$$

where:

$$\Omega = \frac{n^2}{2}(X^2 + Y^2) + \frac{(1-\mu)}{r_1} + \frac{\mu}{r_2} + \frac{\mu A_2}{2r_2^3}\left(1 - \frac{3Z^2}{r_2^2}\right), \tag{2}$$

$$n = \sqrt{\frac{1+3A_2}{2}}, \quad r_1 = \sqrt{(X-\mu)^2 + Y^2 + Z^2}, \quad r_2 = \sqrt{(X-\mu+1)^2 + Y^2 + Z^2} \tag{3}$$

(Sharma and Subba Rao, 1976; Oberti and Vienne, 2003). The oblateness coefficient A_2 is defined as $A_2 = ({R_{\mathrm{E2}}}^2 - {R_{\mathrm{P2}}}^2)/5R^2$, where R_{E2} and R_{P2} are the equatorial and polar radius respectively of the oblate secondary m_2 and R is the distance between the primaries. We place the origin at the secondary and change the scale of lengths by a factor of $\mu^{1/3}$: $X = \mu - 1 + \mu^{1/3}x$, $Y = \mu^{1/3}y$, $Z = \mu^{1/3}z$. Applying these transformations to Ω and setting $A_2 = a_2\mu^{2/3}$ we obtain:

$$\frac{1}{\mu^{2/3}}\left(\Omega - \frac{3}{2}\right) = \frac{3a_2}{4} + \frac{3x^2}{2} - \frac{z^2}{2} + \frac{1}{r} + \frac{a_2}{2r^3} - \frac{3a_2z^2}{2r^5} + \mathcal{O}(\mu^{1/3}), \tag{4}$$

with $r = \sqrt{x^2 + y^2 + z^2}$. Taking the limit of the right-hand side for $\mu \to 0$ we arrive at the potential function:

$$W = \frac{3a_2}{4} + \frac{3x^2}{2} - \frac{z^2}{2} + \frac{1}{r} + \frac{a_2}{2r^3} - \frac{3a_2 z^2}{2r^5}, \tag{5}$$

giving the equations of motion:

$$\begin{aligned} \ddot{x} - 2\dot{y} &= W_x = \left(3 - \frac{1}{r^3} - \frac{3a_2}{2r^5} + \frac{15a_2 z^2}{2r^7}\right)x, \\ \ddot{y} + 2\dot{x} &= W_y = \left(-\frac{1}{r^3} - \frac{3a_2}{2r^5} + \frac{15a_2 z^2}{2r^7}\right)y, \\ \ddot{z} &= W_z = \left(-1 - \frac{1}{r^3} - \frac{9a_2}{2r^5} + \frac{15a_2 z^2}{2r^7}\right)z. \end{aligned} \tag{6}$$

The problem admits a Jacobi integral:

$$2W - (\dot{x}^2 + \dot{y}^2 + \dot{z}^2) = \Gamma, \tag{7}$$

where Γ is the new Jacobi constant related to the Jacobi constant C of the restricted problem by the same relation as in the classical Hill problem:

$$C = 3 + \mu^{2/3}\Gamma. \tag{8}$$

The last three terms of (5) represent a modified Kepler potential, corresponding to a two-body problem where a particle of negligible mass moves under the attraction of a central oblate spheroid whose equatorial plane coincides with the plane of motion. The terms $3x^2/2$ and $-z^2/2$ express a further modification arising from the perturbation of the primary of infinite mass located at infinite distance, according to the Hill problem formulation. The constant term $3a_2/4$ can be omitted, but we choose to keep it here so that (8) retains its simple form. We note that if oblateness of the primary m_1 is also included in the original potential function Ω and the corresponding oblateness coefficient A_1 is scaled in the same way as A_2, then the Hill limiting process produces the same W as above, the oblateness effect of the primary being lost in the process. For coplanar motion ($z = \dot{z} = 0$) W reduces to:

$$W = \frac{3a_2}{4} + \frac{3x^2}{2} + \frac{1}{r} + \frac{a_2}{2r^3}, \quad r = \sqrt{x^2 + y^2}. \tag{9}$$

The problem possesses the same symmetries as the classical Hill problem. For example, if the functions $x = x(t)$ and $y = y(t)$ are a solution, then the functions $x = x(-t)$ and $y = -y(-t)$ are also a solution. In particular, with respect to periodic orbits this means that any periodic orbit of the problem is symmetric to itself or to another periodic orbit with respect to the x-axis. Also, if in Equations (6) we change the signs of x and y the equations remain

invariant, therefore any periodic orbit of the problem is symmetric to itself or to another periodic orbit with respect to the origin. For a fuller discussion of the symmetries involved we refer to Hénon's recent paper on the periodic orbits of the classical Hill problem (Hénon, 2003).

3. Equilibrium Points and Zero-Velocity Curves

3.1. Collinear equilibrium points

The positions of the coplanar equilibrium points are determined by putting the right-hand sides of the equations of motion resulting from (9) equal to zero:

$$3x - \frac{x}{r^3}\left(1 + \frac{3a_2}{2r^2}\right) = 0, \qquad -\frac{y}{r^3}\left(1 + \frac{3a_2}{2r^2}\right) = 0, \tag{10}$$

and solving for x, y. From the second equation we see that for $a_2 \geq 0$ there do not exist equilibrium points out of the x-axis. From the first of (10) for $y = 0$ we have:

$$6r^5 - 2r^2 - 3a_2 = 0, \qquad r = \mid x \mid > 0, \tag{11}$$

which for $a_2 \geq 0$ has exactly one positive root for r, giving two collinear equilibrium points symmetrical with respect to the origin, L_1 on the negative axis and L_2 on the positive axis. Solving this equation approximately we find that these equilibrium points are located at the distance:

$$r_0 = 3^{-1/3} + \frac{3^{1/3}}{2}a_2 - \frac{9}{4}a_2^2 + \frac{11 \times 3^{2/3}}{2}a_2^3 + \mathcal{O}(a_2^4). \tag{12}$$

A more uniform approximation can be obtained in the form:

$$r_0 = 3^{-1/3}\varphi(B), \qquad \varphi(B) = \frac{1 + 53B + 153B^2}{1 + 44B}, \qquad B = \frac{3^{-4/3}}{2}a_2. \tag{13}$$

This can be used to obtain approximately the Jacobi constant value at the collinear equilibrium points as a function of a_2:

$$\Gamma_0 = \frac{3a_2}{2} + 3^{1/3}\left[\varphi(B)^2 + \frac{2}{\varphi(B)} + \frac{18B}{\varphi^3(B)}\right]. \tag{14}$$

The expansion of Γ_0 using (12) on the other hand is:

$$\Gamma_0 = 3^{4/3} + \frac{9}{2}a_2 - \frac{3^{8/3}}{4}a_2^2 + \frac{5 \times 3^{7/3}}{4}a_2^3 + \mathcal{O}(a_2^4), \tag{15}$$

which coincides up to the terms given with the expansion of Γ_0 arising from (14). Note that in the classical Hill problem ($a_2=0$) we have $r_0=3^{-1/3}$ and $\Gamma_0=3^{4/3}$.

To study the stability of L_1 (or L_2) at $(x_0,0,0)$ we place the origin at the equilibrium point by setting $x=x_0+\xi$, $y=\eta$, $z=\zeta$ and linearize the equations of motion obtaining:

$$\ddot{\xi}-2\dot{\eta}=W^{(0)}_{xx}\xi, \qquad \ddot{\eta}+2\dot{\xi}=W^{(0)}_{yy}\eta, \tag{16}$$

$$\ddot{\zeta}=W^{(0)}_{zz}\zeta, \tag{17}$$

where the superscript (0) denotes evaluation at the equilibrium point. The characteristic equation of (16) is:

$$\lambda^4+(4-W^{(0)}_{xx}-W^{(0)}_{yy})\lambda^2+W^{(0)}_{xx}W^{(0)}_{yy}=0, \tag{18}$$

and has roots:

$$\lambda_{1,2}=\pm\theta, \quad \theta=\sqrt{\frac{k_1+9a_2}{6r_0^5}+1}, \quad \lambda_{3,4}=\pm iw, \quad w=\sqrt{\frac{k_1-9a_2}{6r_0^5}-1}, \tag{19}$$

with $k_1=\sqrt{112r_0^4+480r_0^2a_2+549a_2^2}$. To first order terms in a_2 we have:

$$\theta=\theta_0+\frac{3^{8/3}}{4\theta_0}\left(\frac{2}{\sqrt{7}}+1\right)a_2+\mathcal{O}(a_2^2), \quad w=w_0+\frac{3^{8/3}}{4w_0}\left(\frac{2}{\sqrt{7}}-1\right)a_2+\mathcal{O}(a_2^2), \tag{20}$$

where $\theta_0=\sqrt{2\sqrt{7}+1}=2.508\ldots$, $w_0=\sqrt{2\sqrt{7}-1}=2.071\ldots$, are the corresponding quantities of the classical Hill problem. Similarly, the characteristic equation of (17) is:

$$\lambda^2-W^{(0)}_{zz}=0, \tag{21}$$

with roots:

$$\lambda=\pm is, \quad s=\sqrt{4+\frac{3a_2}{r_0^5}}=s_0+\frac{3^{8/3}}{4}a_2+\mathcal{O}(a_2^2), \tag{22}$$

where $s_0=2$ is the corresponding quantity of the classical Hill problem. It follows that the equilibrium points are unstable due to the real roots $\lambda_{1,2}$.

3.2. Out-of-plane equilibrium points

We now consider equilibrium points out of the (x,y) plane. For the right-hand side of the third of Equations (6) to be zero for $z\neq 0$ we must have:

$$-\frac{1}{r^3}-\frac{3a_2}{2r^5}+\frac{15a_2z^2}{2r^7}=1+\frac{6a_2}{2r^5}, \tag{23}$$

and the brackets in the right-hand sides of the first two Equations (6) become:

$$4+\frac{6a_2}{2r^5} \text{ and } 1+\frac{6a_2}{2r^5}.$$

For $a_2>0$ these are positive, therefore any equilibrium points with $z\neq 0$ must have $x=y=0$ and will be located on the z-axis. The equation which determines their position is:

$$r^5+r^2-3a_2=0, \quad r=|z|>0. \tag{24}$$

From this equation we find two equilibrium points at $(0,0,\pm z_0)$, L_z on the positive z-axis and L_{-z} on the negative z-axis. Their distance from the origin is given by:

$$z_0=\sqrt{3}\sqrt{a_2}-\frac{9}{2}a_2^2+\frac{243}{8}\sqrt{3}a_2^{7/2}+\mathcal{O}(a_2^5), \tag{25}$$

while a more uniform approximation of this is:

$$z_0=\frac{4\sqrt{3}\sqrt{a_2}+63a_2^2}{4+27\sqrt{3}a_2^{3/2}}. \tag{26}$$

The expansion of the Jacobi constant value $\Gamma_0=2W(0,0,\pm z_0)$ at these points is:

$$\Gamma_0=\frac{4}{3\sqrt{3}\sqrt{a_2}}-\frac{3}{2}a_2+\frac{9}{2}\sqrt{3}a_2^{5/2}+\mathcal{O}(a_2^4). \tag{27}$$

We note that such out-of-plane equilibrium points have also been found in the restricted three-body problem with oblate primaries, similarly located almost exactly above and below the center of each oblate body (Douskos and Markellos, 2006). We have not checked, however, if their existence might be due to the truncation of the potential employed in deriving the equations of motion.

In order to study the stability of the out-of-plane equilibrium points we work as in the previous section. The corresponding characteristic equations are again (18) and (21) with the partial derivatives now computed at L_z. In this case the roots of (18) are complex of the form:

$$\lambda=\pm\alpha\pm i\beta, \tag{28}$$

with:

$$\alpha=\frac{1}{2}\sqrt{-1-\frac{2}{r_0^5}\left(k_2-\sqrt{-k_2k_3}\right)}, \quad \beta=\frac{1}{2}\sqrt{1+\frac{2}{r_0^5}\left(k_2+\sqrt{-k_2k_3}\right)}, \tag{29}$$

and $k_2 = r_0{}^2 - 6a_2 < 0$, $k_3 = 3r_0{}^5 - r_0{}^2 + 6a_2 > 0$. The expansions of α and β in powers of a_2 are:

$$\begin{aligned} &\alpha = \alpha^\star + \mathcal{O}(a_2^{9/4}), \quad \alpha^\star = (3a_2)^{-3/4} + 2(3a_2)^{3/4}, \\ &\beta = 1 - \frac{3^{7/2}}{32} a_2^{3/2} + \mathcal{O}(a_2^3). \end{aligned} \tag{30}$$

Similarly, the roots of (21) are now:

$$\lambda = \pm i s_z, \qquad s_z = \sqrt{1 - \frac{2k_2}{r_0^5}} = \sqrt{2}\alpha^\star + \mathcal{O}(a_2^{9/4}). \tag{31}$$

We conclude that due to the complex roots (28) the out-of-plane equilibrium points are unstable. We note however that the imaginary roots give rise to periodic straight-line oscillations on the z-axis, which is another feature characteristic of the present problem.

3.3. Zero-velocity curves

The Jacobi integral, for zero velocity, provides the boundaries of the allowed regions of motion. Contours of the surface:

$$\Gamma = \frac{3a_2}{2} + 3x^2 - z^2 + \frac{2}{r} + \frac{a_2}{r^3} - \frac{3a_2 z^2}{r^5}, \tag{32}$$

for values of the Jacobi constant corresponding to the collinear and the out-of-plane equilibrium points are shown in Figure 1 for $z = 0$ (left) and for $y = 0$ (right). We note that the oblateness effect does not essentially change the zero-velocity curves in the (x, y) plane, but new features appear in the (x,z) plane. However, the curves remain symmetrical with respect to both axes as in the classical Hill problem. The first and third row show the two possible topologies of the curves for $a_2 > 0$, while the case of $a_2 \simeq 0.029293$ (middle row) shows the transition from one to the other occurring when $\Gamma(L_1) = \Gamma(L_z)$.

4. Analytical Approximation of the Lyapunov Orbits

We now apply a Lindstedt–Poincaré technique to obtain a third order approximation of the planar periodic orbits emanating from the collinear equilibrium points, the so-called Lyapunov orbits. To do this we transfer the origin at the equilibrium point L_2 by setting: $x = x_{L2} + \xi$, and $y = \eta$. Expanding the equations of motion around L_2 in Taylor series to third-order terms we obtain:

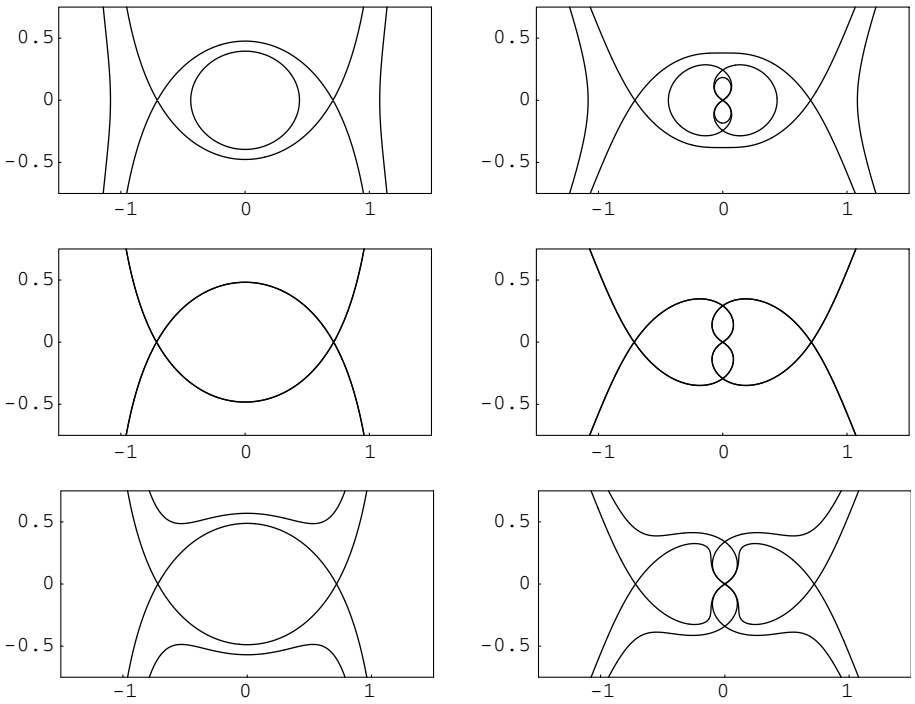

Figure 1. Zero-velocity curves – projections of the zero-velocity surface (32) – in the (x,y) (left) and (x,z) (right) planes for $a_2 = 0.02$, 0.029293 and 0.04 (from top to bottom).

$$\begin{aligned} \ddot{\xi} - 2\dot{\eta} &= P_1^{10}\xi + P_1^{20}\xi^2 + P_1^{02}\eta^2 + P_1^{12}\xi\eta^2 + P_1^{30}\xi^3 = f_1(\xi,\eta), \\ \ddot{\eta} + 2\dot{\xi} &= P_2^{01}\eta + P_2^{11}\xi\eta + P_2^{21}\xi^2\eta + P_2^{03}\eta^3 = f_2(\xi,\eta), \end{aligned} \tag{33}$$

where the coefficients of the powers of ξ, η are constants ultimately depending only on the oblateness coefficient a_2. We seek solutions in the form of the following expansions in powers of an orbital parameter ε:

$$\xi(t) = \sum_{i=1}^{3} x_i(t)\varepsilon^i + \mathcal{O}(\varepsilon^4), \quad \eta(t) = \sum_{i=1}^{3} y_i(t)\varepsilon^i + \mathcal{O}(\varepsilon^4), \tag{34}$$

where

$$\begin{aligned} &x_1(t) = \cos(wt), \quad y_1(t) = s_{11}\sin(wt), \\ &x_2(t) = c_{20} + c_{22}\cos(2wt), \quad y_2(t) = s_{22}\sin(2wt), \\ &x_3(t) = c_{31}\cos(wt) + c_{33}\cos(3wt), \quad y_3(t) = s_{33}\sin(3wt), \end{aligned} \tag{35}$$

while time is "strained" through the transformation $t = (1+E)\tau$, where $E = B_2\varepsilon^2 + \mathcal{O}(\varepsilon^4)$. With τ as the new independent variable System (33) becomes:

$$\begin{aligned}\xi'' - 2(1+E)\eta' &= (1+E)^2 f_1(\xi,\eta),\\ \eta'' + 2(1+E)\xi' &= (1+E)^2 f_2(\xi,\eta).\end{aligned} \tag{36}$$

By substituting (34) into (36) and equating the coefficients of the same powers of ε we obtain the following systems:

$$\begin{aligned}x_1'' - 2y_1' &= P_1^{10} x_1,\\ y_1'' + 2x_1' &= P_2^{01} y_1,\\ x_2'' - 2y_2' &= P_1^{10} x_2 + P_1^{20} x_1^2 + P_1^{02} y_1^2,\\ y_2'' + 2x_2' &= P_2^{01} y_2 + P_2^{11} x_1 y_1,\end{aligned} \tag{37}$$

and a similar system for $x_3(t)$, $y_3(t)$, which is omitted. These are now solved in succession, and the coefficients of the partial solutions (35) are determined as follows:

$$\begin{aligned}s_{11} &= -\frac{P_1^{10} + w^2}{2w} = -\frac{2w}{P_2^{01} + w^2}, \quad c_{20} = -\frac{P_1^{20} + P_1^{02} s_{11}^2}{2P_1^{10}},\\ c_{22} &= -\left[(P_1^{20} - P_1^{02} s_{11}^2)(P_2^{01} + 4w^2) - 4P_2^{11} w s_{11}\right]/P,\\ s_{22} &= -\left[4w(P_1^{02} s_{11}^2 - P_1^{20}) + P_2^{11} s_{11}(P_1^{10} + 4w^2)\right]/P,\end{aligned} \tag{38}$$

where $P = 2P_1^{10}P_2^{01} + 8w^2(P_1^{10} + P_2^{01} + 4w^2 - 4)$ and w is given by (19). The coefficients c_{31}, c_{33}, s_{33} and B_2 are more complicated expressions and are omitted. Alternatively, the coefficients of (35) can be computed to high accuracy as functions of a_2 from the simple expression:

$$\frac{b_0 + b_1 a_2 + b_2 a_2^2}{1 + b_3 a_2 + b_4 a_2^2}, \tag{39}$$

where the numbers b_k, $k = 0,\ldots, 4$ are given for each coefficient in Table I. This provides an accuracy of at least eight decimal places for $a_2 \leq 0.005$. The Lyapunov orbits emanating from L_1 are symmetrical to those emanating from L_2 with respect to the origin and have the same stability properties. These two families are called a and c and one of them (a) is determined numerically in the following section together with the other families of simple-periodic orbits of the problem.

5. Periodic Orbits and their Stability

5.1. The evolution of family characteristics

In a preliminary calculation we have explored numerically the evolution of the families of simple-periodic orbits (symmetric with respect to the x-axis),

TABLE I
The coefficients of (35) computed from (39)

	b_0	b_1	b_2	b_3	b_4
s_{11}	−3.20803719	−36.1377564	−82.9092705	9.76198786	18.6999570
c_{20}	−2.98960402	−46.0437206	−180.620466	13.9651617	45.3561268
c_{22}	1.29967903	21.9679050	86.0737265	12.2727696	34.5300903
s_{22}	0.70950998	−0.34775838	−39.2143688	−1.72703729	−45.6495466
c_{31}	1.80330799	30.0282358	123.294229	21.5952607	120.937665
c_{33}	−1.63735160	0.96609451	231.888475	−5.82504193	−77.5240861
s_{33}	−1.81007007	−0.19173124	142.715373	−3.36796196	−47.9857933
B_2	1.62979242	−63.2066251	−1166.22266	−44.4318288	−419.297882

from the classical Hill case to the present case. To this purpose we have used the Grid search method of Markellos et al. (1974). In Figure 2 we show the effect of oblateness on the network of the family characteristics of simple periodic orbits, including for comparison in Figure 2(a) the network of these characteristics for the classical Hill problem ($a_2 = 0$) given by Hénon (1969). The families a and c are the Lyapunov families discussed above. For $a_2 > 0$ families f and g have a maximum with respect to Γ (not shown), while g' is a "closed" curve (frames (b) and (c)) which branches from family g. Denoting by $g1$ and $g2$ the two critical orbits of g at which g' bifurcates we can observe the eventual disappearance of g' by plotting these two bifurcation points in the (Γ, a_2) plane. This is shown in Figure 3 where the evolution with a_2 of $g1$, $g2$ and of three more horizontally critical orbits of family g is presented. It is seen how $g1$ and $g2$ get closer together as a_2 increases and finally disappear by coalescing with each other at $a_2 \simeq 0.0015$. For larger values of a_2 the basic family g' of the classical Hill problem does not exist.

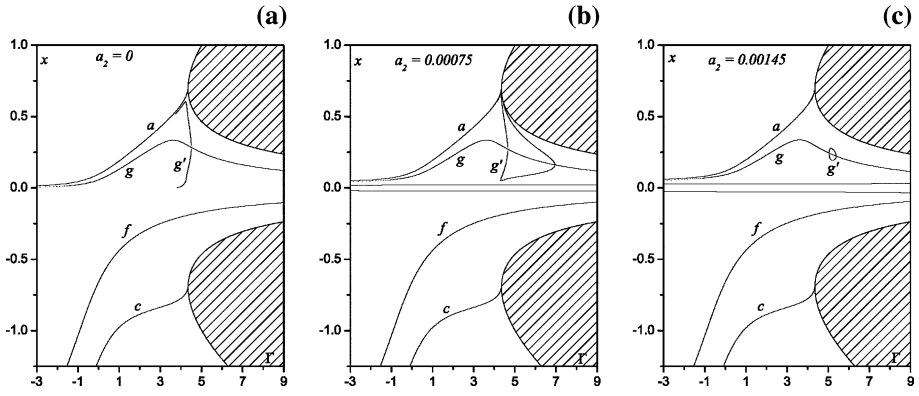

Figure 2. Families of simple periodic orbits in the (Γ, x) plane for sample values of a_2.

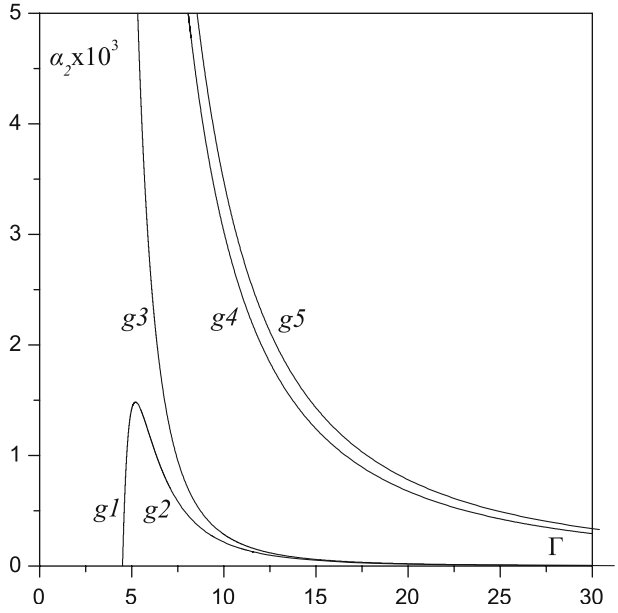

Figure 3. Evolution of horizontally critical orbits of family g for varying a_2.

5.2. Symmetric periodic orbits for $a_2 = 0.005$

The network of the families of simple-periodic orbits, symmetric with respect to the x-axis, was determined numerically with high accuracy calculations of the member orbits and their parameters, for the value of the oblateness coefficient $a_2 = 0.005$. The characteristic family curves of the basic families in the (Γ, x) plane are given in Figure 4. The orbits of each family are shown in Figures 5 and 6. The specific members plotted are represented by dots on the characteristic curve of each family. The basic families f and g consist of orbits symmetric with respect to both axes as in the classical problem.

The iso-energetic stability parameters are computed accurately using the equations of variation and the relevant formulae of Markellos (1976):

$$\begin{aligned}
a &= \frac{\partial x}{\partial x_0} + \frac{\partial x}{\partial \dot{y}_0} D_1 + D_2 \left(\frac{\partial y}{\partial x_0} + \frac{\partial y}{\partial \dot{y}_0} D_1 \right), \\
b &= \frac{\partial x}{\partial \dot{x}_0} + \frac{\partial x}{\partial \dot{y}_0} D_2 + D_2 \left(\frac{\partial y}{\partial \dot{x}_0} + \frac{\partial y}{\partial \dot{y}_0} D_2 \right), \\
c &= \frac{\partial \dot{x}}{\partial x_0} + \frac{\partial \dot{x}}{\partial \dot{y}_0} D_1 - \frac{\ddot{x}_0}{\dot{y}_0} \left(\frac{\partial y}{\partial x_0} + \frac{\partial y}{\partial \dot{y}_0} D_1 \right), \\
d &= \frac{\partial \dot{x}}{\partial \dot{x}_0} + \frac{\partial \dot{x}}{\partial \dot{y}_0} D_2 - \frac{\ddot{x}_0}{\dot{y}_0} \left(\frac{\partial y}{\partial \dot{x}_0} + \frac{\partial y}{\partial \dot{y}_0} D_2 \right),
\end{aligned} \tag{40}$$

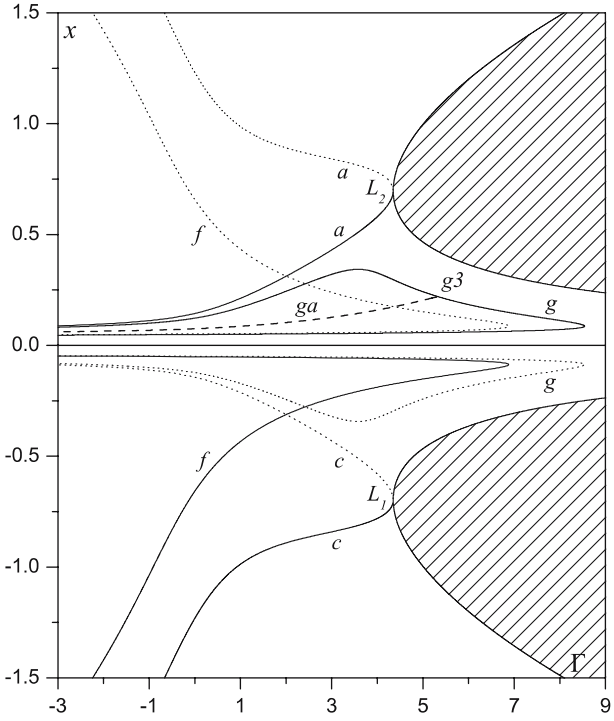

Figure 4. Characteristics of families of periodic orbits in (Γ,x) plane for $a_2 = 0.005$. Regions not allowed to motion are shown hatched. Continuous lines: positive crossings of the x-axis, dotted lines: negative crossings. The projection in this plane of family *ga* (see Section 5.3) is also shown (dashed line).

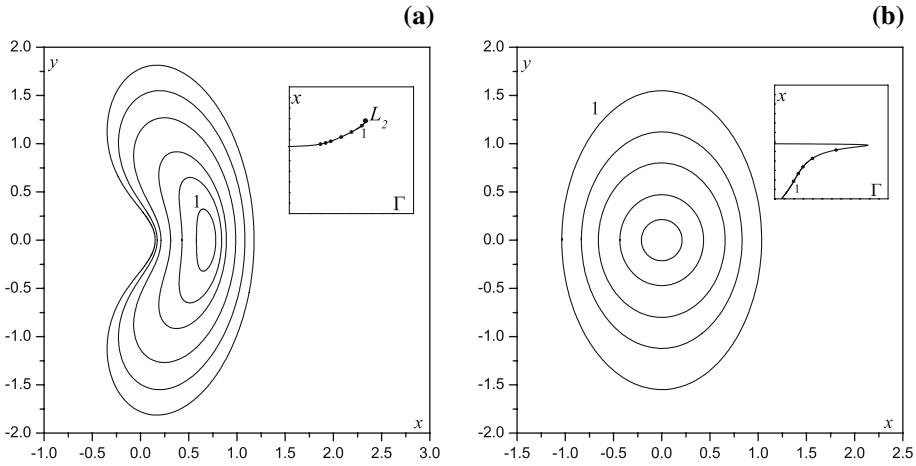

Figure 5. Typical orbits of the Lyapunov family *a* (left) and family *f* of retrograde satellites (right).

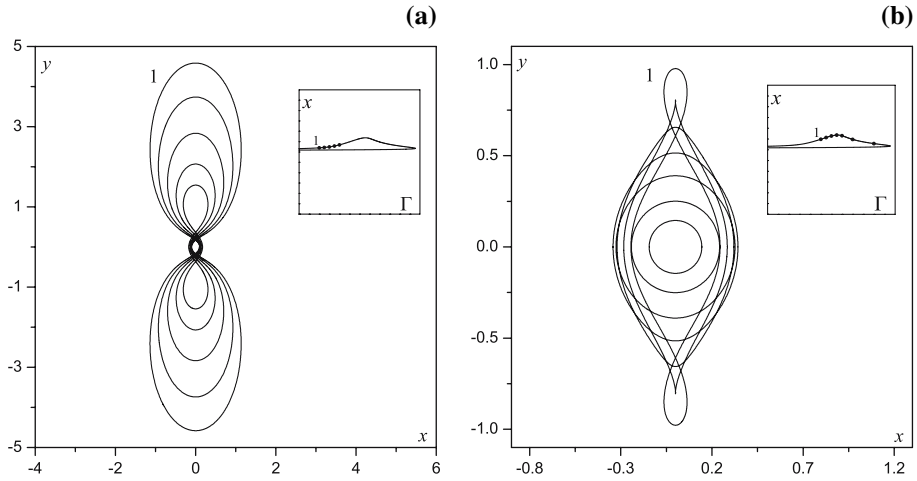

Figure 6. Typical orbits of family g of direct satellites. Evolution phases (a) and (b).

where

$$D_1 = \frac{1}{2\dot{y}_0}\frac{\partial \Gamma_0}{\partial x_0}, \quad D_2 = -\frac{\dot{x}_0}{\dot{y}_0}. \tag{41}$$

The horizontal and vertical stability diagrams of the basic families are given in Figure 7. Because of the large values of the horizontal stability parameter we plot the quantity $\sinh^{-1} a = \ln(a + \sqrt{a^2+1})$ instead of a, and similarly for a_v. In the case of the Lyapunov families a and c the limiting values of the horizontal and vertical stability parameters a and a_v are given by:

$$a = \cosh(2\pi\theta/w), \quad a_v = \cos(2\pi s/w), \tag{42}$$

(Hénon, 1969, 1973), where θ, w and s are given by (19) and (22). The effect of oblateness on these limiting values is given to first order terms in a_2 by:

$$a = \cosh\left(\frac{2\pi\theta_0}{w_0}\right) + \frac{3^{8/3}\pi}{w_0^3\theta_0}\left[\left(\frac{1}{2} - \frac{1}{\sqrt{7}}\right)\theta_0^2 + \left(\frac{1}{2} + \frac{1}{\sqrt{7}}\right)w_0^2\right]\sinh\left(\frac{2\pi\theta_0}{w_0}\right)a_2,$$
$$a_v = \cos\left(\frac{2\pi s_0}{w_0}\right) - \frac{3^{8/3}\pi}{w_0^3}\left[\left(\frac{1}{2} - \frac{1}{\sqrt{7}}\right)s_0 + \frac{1}{2}w_0^2\right]\sin\left(\frac{2\pi s_0}{w_0}\right)a_2. \tag{43}$$

The horizontal and vertical critical orbits of the basic families are given in Tables II, III and IV. In the last column we give the quantity being zero at the critical orbit and characterizing the type of bifurcation. For details on the

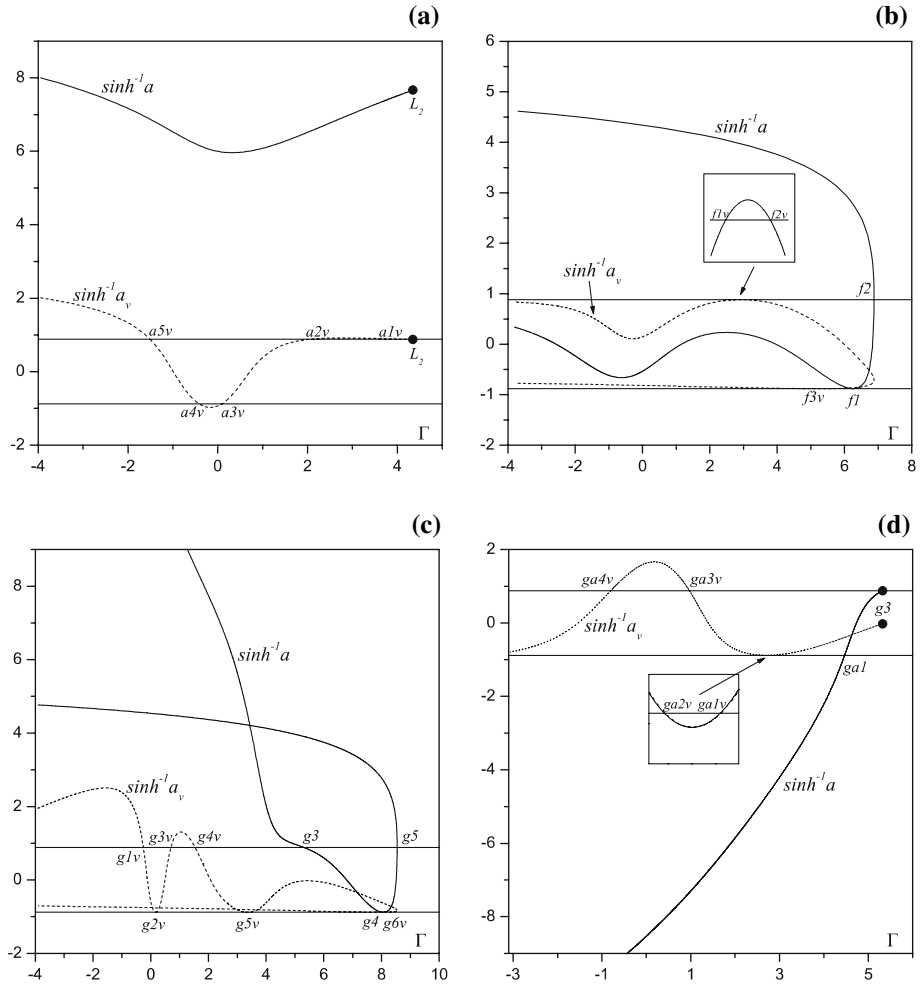

Figure 7. Horizontal and vertical stability curves of the families *a* (a), *f* (b), *g* (c) and *ga* (d).

TABLE II
Family *a*.

	$T/2$	x_0	x_1	$\dot{y}_0$	Γ	
*a*1*v*	3.77261823	0.10283840	1.87072706	5.05928300	−1.51181748	B_v
*a*2*v*	3.20825731	0.12738525	1.39025705	4.31085150	−0.40798507	D_v
*a*3*v*	2.82053403	0.14843241	1.20048371	3.87138301	0.08905300	A_v
*a*4*v*	1.82538508	0.31775198	0.88757084	2.16921761	2.05496063	B_v
*a*5*v*	1.53371074	0.61103543	0.76354199	0.52710647	4.14480078	C_v

TABLE III
Family f.

	$T/2$	x_0	$\dot{y}_0$	Γ	
$f1v$	0.33711337	−0.24977300	2.38849869	2.81787740	C_v
$f2v$	0.31233242	−0.23730792	2.44086487	3.02063167	B_v
$f3v$	0.02995807	−0.06401100	6.71389916	5.25163175	A_v, D_v
$f1$	0.09328264	−0.11381020	3.84063326	6.26078119	A, D
$f2$	0.05568796	−0.08663841	4.89103343	6.88070443	C

TABLE IV
Family g.

	$T/2$	x_0	$\dot{y}_0$	Γ	
$g1v$	4.75505815	0.11511093	4.57762728	−0.25478849	B_v
$g2v$	4.21134576	0.12916700	4.20545585	0.17566943	A_v, D_v
$g3v$	3.45718972	0.15368836	3.71085169	0.69864588	B_v
$g4v$	2.51197020	0.20884921	2.95301408	1.54322169	C_v
$g5v$	1.27803439	0.33953097	1.73084919	3.37572522	A_v, D_v
$g3$	0.34254885	0.22021004	2.09276319	5.32378720	B
$g6v$	0.03814351	0.07099514	5.84923391	7.95284807	A_v, D_v
$g4$	0.09323314	0.11022786	3.72217763	8.06690362	A, D
$g5$	0.05773470	0.08663645	4.71791006	8.54528426	C

definitions of horizontal and vertical stability parameters and the types of critical orbits (and resulting bifurcations) we refer to Hénon (1965, 1973).

We note in particular that if $a=1$ and $b=0$ (equivalently $B=0$) we have a bifurcation with a family of simple periodic orbits non-symmetric with respect to the x-axis. This type of bifurcation does not occur for the families of simple periodic orbits of the classical Hill problem, but occurs in the present problem at the critical orbit $g3$ of the basic family g of direct satellites. We further note that the critical orbit $g4$ marks the bifurcation from family g of a family of double-periodic symmetric orbits, while $g5$ is the orbit of maximum Γ along the family g, and similarly for the critical orbits $f1$ and $f2$ of family f. The evolution of these critical orbits for varying a_2 has been shown in Figure 3.

5.3. Periodic orbits non-symmetric w.r.t. the x-axis

An important feature of this problem is the existence of a family of simple non-symmetric periodic orbits (with respect to x-axis). This family bifurcates from family g at the horizontally critical orbit $g3$ and consists of orbits

symmetric with respect to the y-axis. The characteristic of this family computed as a family of asymmetric periodic orbits with respect to the x-axis cannot be represented in the (Γ,x) plane because it is a three-dimensional curve in the ($\Gamma, x, \dot{x}$) space, but we have plotted in Figure 4 its projection in the (Γ,x) plane for $a_2 = 0.005$. It follows from the symmetry properties discussed in section 2 that for any asymmetric periodic orbit with respect to the x-axis another orbit exists which is symmetric with the first one with respect to the x-axis. Therefore at $g3$ two branches of a family of asymmetric periodic orbits bifurcate from g which are named here ga and ga' (but we may refer to both branches collectively as the two-branch family ga). The evolution of these branches as a_2 increases from the classical case ($a_2 = 0$) is shown in Figure 8 where the family characteristics are plotted in the (Γ, y) plane, and a log scale is used for the Γ values. The Grid search of Markellos et al. (1974) was now employed in the (Γ,y) plane and the orbits of all families shown have been recomputed as symmetric with respect to the y-axis.

The branches ga and ga' were found only for non-zero oblateness of the secondary. Their orbits are shown in Figure 9, where the orbits of ga are drawn with continuous lines and those of ga' with dotted lines. As the orbits evolve away from the bifurcation orbit $g3$ (marked by 1 in frame (a) of Figure 9), they develop loops and become double-periodic in the sense that they possess four intersections with the y-axis (frame (b) of Figure 9). In Figure 7 (d) we have given the horizontal and vertical stability curves of the branch ga, while the horizontal and vertical critical orbits of this are given in Table V. The critical orbits of ga' can be obtained from those of ga by symmetry with respect to the x-axis. The importance of these branches of non-symmetric with respect to the x-axis orbits is enhanced by the fact that in their initial segments they consist of orbits which are horizontally (and vertically) stable. In fact, their orbits are quite dominant elliptic points in the sense that they are surrounded by invariant curves covering a substantial

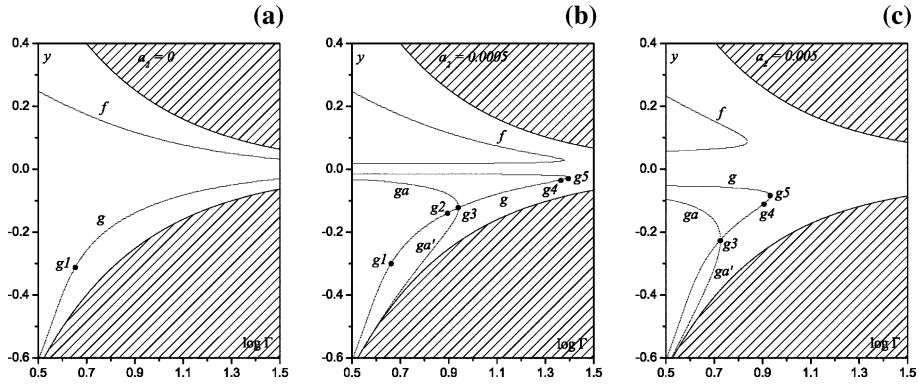

Figure 8. Characteristics of families of simple periodic orbits in the (Γ, y) plane for sample values of a_2. Hatched regions are not allowed to motion.

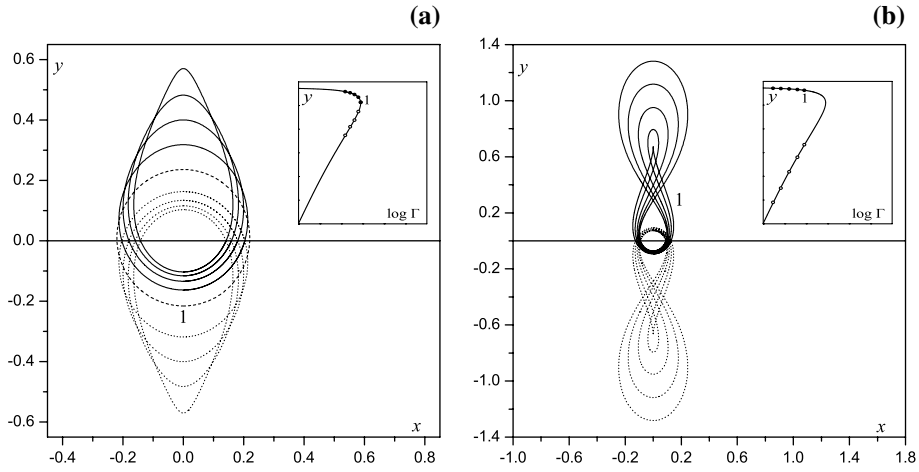

Figure 9. Typical orbits of the branches *ga* and *ga′* for $a_2 = 0.005$. Evolution phases (a) and (b). In frame (a) marked by 1 is the bifurcation orbit *g*3.

TABLE V
Family *ga*.

	$T/2$	y_0	y_1	$\dot{x}_0$	Γ	
*ga*1	0.43622113	−0.13219990	0.40674490	3.58233415	4.46708384	A
*ga*1*v*	0.74273891	−0.08912669	0.72758524	5.17203381	2.75984347	A_v
*ga*2*v*	0.77267904	−0.08733259	0.75682040	5.26995641	2.64257865	D_v
*ga*3*v*	1.46936383	−0.06905086	1.51961100	6.57177877	0.97005938	C_v
*ga*4*v*	2.58957899	−0.05926378	4.21806840	7.65355894	−0.80043307	B_v

region on the surface of section. This appears in their Poincaré surface of section portraits in the $(x, \dot{x})$ and $(y, \dot{y})$ planes shown in Figure 10. The two-branch family *ga* plays a role similar to that of family *g′* in extending the distance at which stable direct periodic satellites may exist when the family *g* itself does not consist of stable orbits.

6. Conclusions

We have introduced a three-dimensional version of Hill's problem with oblate secondary and considered its main dynamical features. We determined the equilibrium points and their stability and explored numerically the network of its families of simple periodic orbits in the plane paying special attention to the evolution of these families from the classical Hill problem. Our main results characteristic of the present problem are as follows. The basic families *g* and *f* of direct and retrograde periodic satellite orbits consist

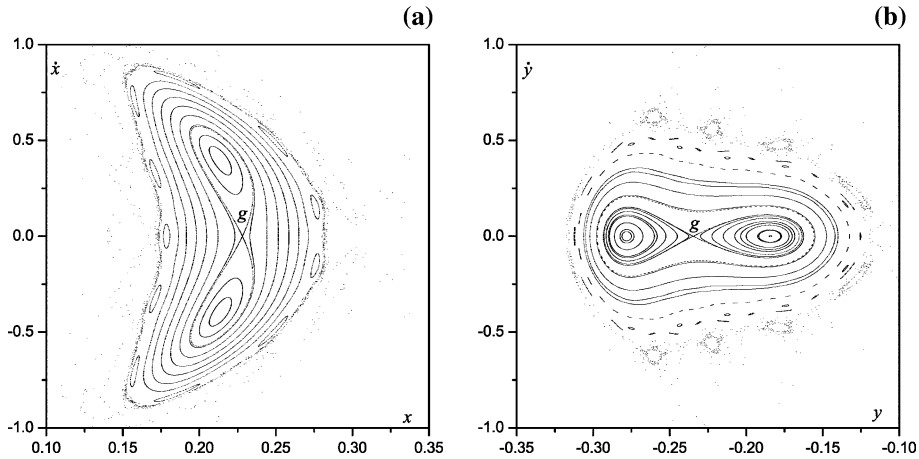

Figure 10. Poincaré surface of section portraits for $a_2 = 0.005$ and $\Gamma = 5.2$ in the $(x, \dot{x})$ and $(y, \dot{y})$ planes. The elliptic points at the centers of the two dominant islands of invariant curves represent the stable periodic orbits ga and ga', while the hyperbolic point g represents the unstable orbit of family g.

of two branches each, and do not exist for infinitely large values of the Jacobi constant Γ as they do in the classical problem, but only up to finite maximum values depending on the value of the oblateness coefficient. For non-zero values of the oblateness coefficient a_2 the basic family g' of the classical problem closes upon itself; its two bifurcation orbits with family g get closer to each other as a_2 increases and eventually disappear by coalescing with each other for $a_2 \simeq 0.0015$. Also, for $a_2 > 0$ the present problem possesses out-of-plane equilibrium points, as well as a two-branch family of stable simple-periodic plane orbits non-symmetric with respect to the x-axis, although symmetric with respect to the y-axis, features which do not exist in the classical problem. The family of non-symmetric orbits plays a similar role to that of family g' in extending the distance at which stable direct periodic satellites may exist when the family g itself does not consist of stable orbits.

Acknowledgment

During this work one of the authors (A.E.P.) was in receipt of a "K. Karatheodory" research grant.

References

Douskos, C. N. and Markellos, V. V.: 2006, *Astron. Astrophys.* **446**, 357.

Gurfil, P. and Meltzer, D.: 2005, 25th *Israeli Annual Conference on Aerospace Sciences*, Preprint.

Hamilton, P. P. and Krivov, A. V.: 1996, *Icarus* **123**, 503.
Hénon, M.: 1965, *Ann. Astrophys.* **28**, 992.
Hénon, M.: 1969, *Astron. Astrophys.* **1**, 223.
Hénon, M.: 1973, *Astron. Astrophys.* **28**, 415.
Hénon, M.: 2003, *Celes. Mech. Dyn. Astron.* **85**, 223.
Kanavos, S. S., Markellos, V. V., Perdios, E. A., and Douskos, C. N.: 2002, *Earth, Moon Planets* **91**, 223.
Markellos, V. V., Black, W., and Moran, P. E.: 1974, *Celes. Mech.* **9**, 507.
Markellos, V. V.: 1976, *Astrophys. Space Sci.* **43**, 449.
Markellos, V. V., Roy, A. E., Velgakis, M. J., and Kanavos, S. S.: 2000, *Astrophys. Space Sci.* **271**, 293.
Markellos, V. V., Roy, A. E., Perdios, E. A., and Douskos, C. N.: 2001, *Astrophys. Space Sci.* **278**, 295.
Oberti, P. and Vienne, A.: 2003, *Astron. Astrophys.* **397**, 353.
Sharma, R. K. and Subba Rao, P. V.: 1976, *Celes. Mech.* **13**, 137.
Sharma, R. K.: 1987, *Astron. Astrophys.* **135**, 271.